Vacuum-ultraviolet emission from rare-gas impurities in alkali metals

P. N. First* and C. P. Flynn
Department of Physics, 1110 West Green Street, University of Illinois at Urbana-Champaign, Urbana, Illinois 61801
(Received 20 October 1989; revised manuscript received 23 April 1990)

Photon emission spectra from the $np^5(n+1)s \rightarrow np^6$ transitions of core-excited Kr ($n=4$) and Xe ($n=5$) impurities in host alkali metals are reported. A band arising from the decay of single rare-gas atoms is identified, as well as features characteristic of interaction between neighboring impurity atoms. Lifetimes determined from emission intensities relative to the analogous core excitation in the host metal were found to be roughly constant at ~ 5 meV in all the alloys studied. The Lorentzian component of the emission edge is considerably wider at almost 200 meV. These model systems have previously been studied in absorption where an anomalously broad and suppressed Fermi edge was found, in contrast to the predicted "x-ray-edge" singularity. Emission results for isolated impurities show small overlap with the corresponding absorption edges, and the usual mirror symmetry of the two edges is entirely absent. The effect of configuration interaction is discussed as a possible explanation for the anomalous absorption threshold, rather than shakeup from conduction-electron recoil as previously supposed.

I. INTRODUCTION

This paper reports measurements of vacuum-ultraviolet (vuv) photon emission from core-excited rare-gas atoms in alkali-metal lattices. Spectra due to the $np^5(n+1)s \rightarrow np^6$ radiative transitions of Kr ($n=4$) and Xe ($n=5$) alloyed into K, Rb, and Cs metals have been acquired. The results are compared with corresponding absorption spectra as well as the emission band from $np^5(n+1)s^2 \rightarrow np^6(n+1)s$ transitions in the host metal. Most of the samples studied were dilute alloys, so that the properties approached those of materials in which the rare-gas centers were single impurities isolated in the metal matrix. Interest focuses on electronic structures of the ground and excited states probed by these measurements, and on the transient disturbance of the conduction electrons caused by the optical event. The emission results point to a new interpretation of the anomalous line shapes found earlier in absorption studies of similar alloys.

The interactions of rare-gas atoms with metals have previously been selected for study in the anticipation that their chemical simplicity would lead to model properties that are readily understood. Instead, experiments in three areas have revealed unexpectedly rich structure. Mignolet[1] and others[2] adsorbed rare gases on metals at low temperature and discovered surprisingly large work function changes in some cases. In connection with related measurements of adsorbate excitation spectra,[3] this behavior has been interpreted using many-body perturbation theory,[4] the interpretation rejected from one-electron arguments,[5] and later reaffirmed[6,7] without a universally agreed explanation emerging. In a second area, rare-gas atoms were quench condensed into Hg by Raz, Gedanken, Even, and Jortner[8] and into alkali metals by Phelps *et al.*[9] to study electronic transport, and by Tilton *et al.*[10,11] to examine the outer core-excitation spectra. The observed conductivity could be modeled reasonably by percolation, but the core-excitation spectra contradict accepted theoretical models so strongly that the results are no longer discussed in contemporary reviews of "x-ray-edge" behavior. The results are nevertheless confirmed by later studies of rare-gas atoms adsorbed at low coverage on alkali-metal surfaces.[12] The threshold behavior of the adsorbed species resembles that in the bulk, and "pair lines" proportional to the concentration of impurity pairs are seen in both cases. Finally, a great deal of effort has recently been directed to the growth of well-ordered rare-gas overlayers on carefully prepared metal single-crystal surfaces.[13,14] Spectroscopic investigations have revealed detailed layer-specific structure. However, the origins of the work function behavior still remain a subject of controversy.

Our focus in the present research is on the second of these areas, specifically, the core spectroscopy of rare-gas atoms embedded in a simple metal matrix typified by the alkali metals. A broad and apparently reliable understanding of the rare-gas structure in the metal has evolved. In the ground state, conduction electrons are repelled from the already-neutral rare-gas cell and the scattering from simple models that satisfy screening requirements is consistent with the observed residual resistance.[9] The relaxed excited state of the rare-gas atom is expected to be particularly simple because the core-excited rare gas has an electronic structure almost identical to the ground state of its neighboring alkali metal in the periodic table. These approximate chemical ideas are fully confirmed by their ability to predict accurately (to $\sim 2\%$) the excitation thresholds of the rare-gas cores in the metallic environment.[10] They also predict the changes of conduction-electron phase shifts that occur when the rare-gas atom is excited. These values have recently been confirmed by detailed electronic structure calculations from Meltzer, Pinski, and Stocks.[15] Thus, the basic structural aspects of the rare-gas centers appear

to be reasonably well understood for both the ground and excited states.

The observed excitation spectra of rare-gas atoms coupled to alkali metals, both as impurities in the bulk and as adsorbates on surfaces, nevertheless present a major challenge to current theories. The Mahan-Nozieres-DeDominicis (MND) theory[16–19] predicts the threshold absorption behavior above the relaxed energy E_t as a power law $\sim(\hbar\omega - E_t)^{-\alpha}$, $(\hbar\omega > E_t)$ with the exponent α fixed by the phase shift changes between the ground and excited configurations. Calculations for host alkali-metal atoms[20,21] give values of $\alpha \sim 0.3$ that reproduce observed peaks at the pure metal absorption thresholds in a semiquantitative way. The problem is that for rare-gas impurities the chemical estimates, now precisely confirmed by detailed theory,[15] predict much the same exponent as for the alkali-metal cores. Unfortunately the experiments contradict the prediction. Systematically for Xe and Kr with several alkali-metal hosts, both on the surface[12] and in the bulk,[10] the rare-gas spectra indicate $\alpha \sim -1$. That is, the spectra start from zero at a suppressed threshold, rather than exhibiting the expected "MND anomaly" at E_t. It has not proved possible to explain this contradiction as the result of some unidentified broadening, in part because the threshold energy agrees with that calculated from the chemical modeling described above. Several theoretical efforts have failed to provide a satisfactory description of the absorption line shape.[22–24]

Among alternative spectroscopies, measurements of electron-induced emission appear to offer an attractive approach to these problems. The difficulty with spectroscopies such as photoemission that rely on electron energies for resolution is that rapid scattering restricts the useful probe depth to a few monolayers. This surface specificity can lead to problems arising from surface segregation when dilute alloys are investigated. Photon-induced emission also seems a useful future probe. In the present research, the relaxed core-excited state created by electron beam excitation is studied by means of the photon emitted when a core hole recombines, much as in Skinner's[25] original emission experiments. This permits an independent determination of E_t to compare with that observed from absorption and theory. It also affords an alternative characterization of the x-ray-edge behavior, which is generally expected to be much the same in absorption and emission. A particular interest is attached also to the general shape of the emission band, since the excited-state conduction-electron distribution is predicted to be an almost uniform electron liquid.

Emission experiments were undertaken on rare gases in alkali-metals using equipment that has recently been used to study pure alkali metals[26] and alkali-metal impurities in alkali metals.[27,28] Methods have been developed with this apparatus to determine the relative total emission from two different atoms in the sample, and hence to determine the core-hole lifetimes in favorable cases. This newly developed technique added further interest to the chosen investigations. In what follows, relevant experimental matters are briefly reviewed in Sec. II, and Sec. III reports the measurements made on Kr and Xe alloyed into Cs, Rb, K, and Na. Section IV analyzes and discusses these data, and Sec. V contains a brief summary of the conclusions.

II. EXPERIMENT

Several characteristics of the rare-gas–alkali-metal system combine to make emission studies difficult. The alkali metals are highly reactive so that careful vacuum arrangements are necessary if the samples are to remain uncontaminated for a suitable time. Still more difficult is the fact that alkali metals and rare gases exhibit negligible equilibrium solubility. As in previous research, it was therefore essential to prepare samples *in situ* by quench condensation on a substrate held near liquid He temperatures. Under these experimental conditions the heat input from the electron beam used to excite the core holes presents further design problems.

An apparatus that satisfies these requirements has been described in an earlier publication,[26] to which the reader is referred for details. In brief, a 2-keV electron beam was focused to a spot size ~ 100 μm for optimum source brightness, given the limited power input permitted by the cryogenic arrangements. The sample so excited was positioned at the first focus of a $f/0.5$ ellipsoidal mirror that matched the light optimally into a $f/4.5$ UHV monochromator. Detection took place using a CsI coated microchannel plate and charge-coupled-device (CCD) array detector, or else with a sodium salicylate scintillator screen and CCD for spectra in the energy range below ~ 7 eV where CsI has no sensitivity. A LiF filter could be placed in the optical path to attenuate photons above 11.8 eV, thus eliminating distortions from higher-order diffraction in many cases. The substrate itself was a 1-mm-diam copper rod that conducted heat efficiently to a heat sink on an inner cryo-can cooled by a Helitran cold finger. It was possible to maintain the substrate at temperatures down to 12 K in the presence of < 10 mW power load from electron beam heating. The temperature was monitored by a thermocouple and a carbon resister attached to the sample assembly.

Rare-gas–alkali-metal alloys were prepared by simultaneous deposition of the components onto the cold substrate. This leads to continuous, high-density films with well-controlled resistances, as described in detail elsewhere.[9] These unstable materials are known to evolve towards thermal equilibrium above ~ 20 K. Care was therefore taken to grow and subsequently maintain the samples well below this critical temperature, in order that the rare-gas atoms retained essentially random site occupancies throughout the lattice. The pure alkali metals were obtained from evacuated glass ampules as provided by the manufacturer. The ampule was crushed in UHV and heated to provide a molecular beam along a carefully collimated path. Calibrated quartz crystals placed beside the path to the substrate were used to monitor the alkali fluxes in order that the composition could be measured precisely. The rare-gas molecular beam originated at a fine nozzle, and was fed through UHV tubing from a buffer volume equipped with an absolute pressure gauge, to which pure gases could be supplied directly from small storage bottles. By placing a quartz crystal monitor at

the sample position, the gas flux as a function of backing pressure was carefully determined in a separate experiment.

For studies of alloys less than ~8 at. % rare gas, reabsorption of emitted radiation was unimportant for any of the features of interest, but above this concentration attenuation from the strong rare-gas absorption band could significantly affect emission intensities of both the host alkali-metal band and the "pair peaks" described below. In order to quantify these intensities relative to the main rare-gas band, samples were often fabricated with a restricted amount of impurity atoms. In what follows, "thick sample" will refer to those of sufficient thickness to fully attenuate the incident electron beam, while "thin samples" free of reabsorption effects were prepared with a total rare-gas deposition of $(6-7)\times 10^{15}$ atoms/cm^2 (integrated over sample depth). That part of the electron beam not stopped by the sample in this case was absorbed by an underlying layer of silver, which also contributed some slowly varying background emission.

Another point that warrants specific mention is the charging and heating observed for samples with compositions near to or past the metal-insulator transitions. These are consequences of the electron beam interaction with samples that are poor electrical and thermal conductors. Under some operating conditions, such materials were observed to evolve irreversibly and even to evaporate from excess heating. This was accommodated for the results reported here by reducing the electron beam current. Good signals could be obtained from concentrated alloys with currents below 0.5 μA (<1 mW total power), as compared with the 1–4 μA currents generally employed for more dilute alloys.

III. RESULTS

Xe spectra occur near 7 eV, in a difficult spectral region through which the CsI photocathode of our microchannel plate cuts off. These same problems persist to some extent even for Kr spectra, which extend from about 9.5 down to 7 eV. Figure 1 shows for 2 at. % alloys of Kr in Rb and Cs the type of background subtractions that must be made in the more dilute samples. These subtractions are substantial and they coincide with the CsI cutoff. The Kr edge structure near 9 eV is nevertheless detected unambiguously, and the distribution of strength in the long emission tail down to 6.5 eV is clearly determined. In more concentrated alloys, of course, the rare gas emission becomes more intense and its detectability improves. For Xe the cutoff made accurate subtractions so difficult, other than at the emission edge itself, that recourse was made to a sodium salicylate phosphor in conjunction with the CCD detector. The loss of detection efficiency was partly compensated by the featureless spectral response of sodium salicylate, which enhanced signal visibility. The agreement between spectra taken by the two methods is documented below.

It is important to note at this point that the spectra are generally composites of three or more overlapping sections matched throughout those regions in common. The grating dispersion was such as to allow only a 450-Å-wide

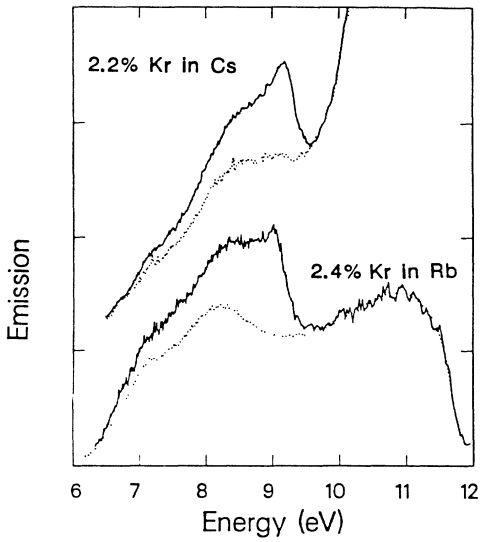

FIG. 1. Spectra of Kr impurities near the dilute limit in Rb and Cs host lattices. Solid lines correspond to the raw spectra while dotted lines show the background due to emission from the pure alkali metal. Note the CsI detector cutoff below 7 eV and attenuation above 11.8 eV caused by the LiF filter.

band to lie on the array detector for any given grating position, insufficient to cover the entire spectral range required. Since more integration time was generally allowed for that section which included the emission threshold, the signal-to-noise ratio in these portions of the spectra is correspondingly better than the signal-to-noise in, for example, the band tails. The emission data presented here have not been smoothed in any way, except for binning adjacent points from the raw spectrum to produce the displayed point density. Overall resolution was <70 meV at the rare-gas emission thresholds and unless otherwise noted, the spectra are presented as intensity per unit energy, i.e., the raw data has been divided by E^2 to correct for constant *wavelength* resolution of the spectrometer.

The best data were taken for Kr in Rb. Figure 2 shows Kr N_{23} spectra taken at four different Kr concentrations. Spectra from the more dilute alloys define the emission of Kr atoms effectively isolated from each other in the Rb metal environment. It is apparent that the approximately normalized spectra for 5.5 and 2.4 at. % agree very well, so the effects of Kr-Kr interactions on the main band are not important. The emission band has a long tail, somewhat like that of the alkalis.[26] Unlike the alkali metals, however, the threshold (Fermi edge) is not sharp, but exhibits a distinct Lorentzian-like breadth. In contrast with this general edge width the emission peak is extremely sharp, and remains so for 2 up to 19 at. %. This is an important matter to which we return in the discussion of Sec. IV. We note further that the N_2 spin-orbit partner emission is absent from its expected location 0.6 eV above the N_3 edge. By including N_2 emission in the model fits described in Sec. IV we determined that this contribution could be as much as 6 at. % of the total N_3 intensity and still remain unobservable due to Coster-

Kronig lifetime broadening. Two small, sharp peaks are, however, visible at higher concentrations between 10 and 11 eV, separated by the spin-orbit splitting. These are "pair peaks" of the type observed earlier in absorption spectra from similar alloys.[11] The spectra in Fig. 2 are from thick films, so the magnitude of these features is affected by reabsorption for the 19 and 61 at. % samples, as mentioned in Sec. II. At the highest Kr concentrations a large peak near 8.4 eV overwhelms the metal edge emission. This undoubtedly arises from recombination events that take place in regions so Kr rich that the excitation process is partly decoupled from the metallic environment.

Comparable results for Kr in Cs and Kr in K are presented in Figs. 3 and 4. The 7 and 14 at. % alloys in Cs yield spectra that strongly resemble the Rb data of Fig. 2. Problems of background subtraction mar the data for 2.2 at. % Kr but the shape of the edge, including the general width and peak shape, remain unambiguously defined; the features near 6.5 and 8.4 eV on the long tail of the 2.2 at. % spectrum are not, however, real. The strong peak at 8.3 eV in the 42 at. % Kr–Cs alloy, also faintly visible at 25 at. % Kr, must arise from precisely the same causes mentioned above for Rb. All these features recur also for Kr in the K lattice (Fig. 4) where the more reliable spectra show similarly long low-energy tails. Background subtraction again causes problems in the tail of the most dilute alloy. Small pair peaks are clearly visible at high concentrations.

The results shown in Fig. 5 for Xe emission from Xe–Cs alloys are taken with a sodium salicylate phosphor as explained in Sec. II. It must be noted that these spectra were acquired early on at substantially higher beam current (30 μA) than was used for any of the others presented. Nevertheless, the basic features were later reproduced at much lower currents, but with consequently more noise. The Xe spectrum has an edge near 7.5 eV similar in shape to the Kr Fermi edge shown in Figs. 2–4, but the band as a whole is substantially narrower. For the 7 at. % alloy the statistics are sufficient to estab-

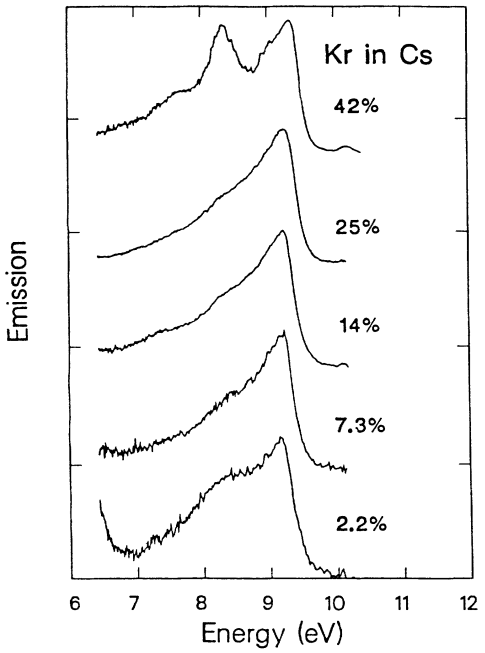

FIG. 3. Emission spectra for various concentrations of Kr in Cs after subtraction of the pure metal background. The data are from thick films using the CsI detector.

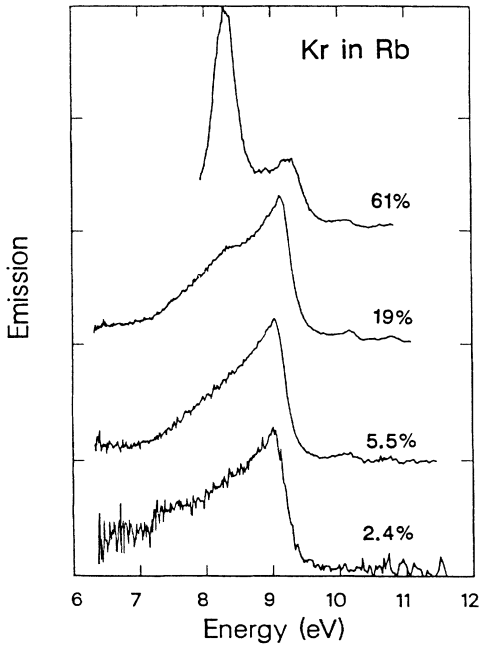

FIG. 2. Emission spectra for various concentrations of Kr in Rb after subtraction of the pure metal background. The data presented are from thick films, as described in the text, using the CsI detector.

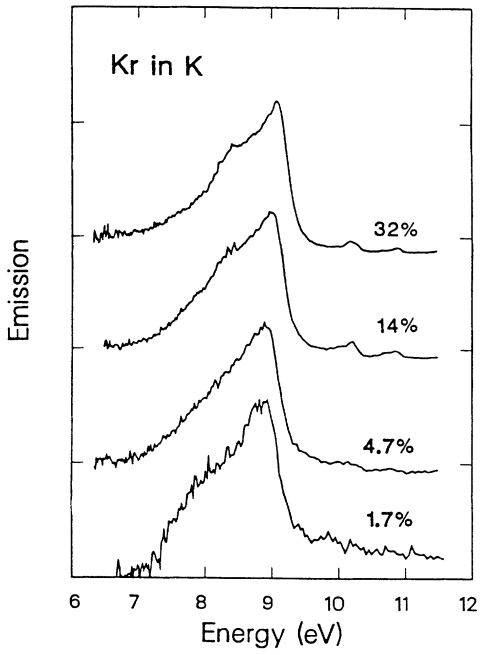

FIG. 4. Emission spectra for various concentrations of Kr in K after subtraction of the pure metal background. The data are from thick films using the CsI detector.

lish that the edge is largely unchanged from 16 at. % but finer details are quite uncertain.

An important characteristic of these spectra is their overlap with comparable absorption spectra. Figures 6 and 7 show this overlap for Kr and Xe spectra respectively. For Kr in Fig. 6 the overlap between absorption and emission in Na, K, Rb, and Cs host lattices is quite interesting. Without exception, the curves cross well below their half height, and the overlap occurs in the region of 9.2 ± 0.2 eV where the relaxed electronic threshold is predicted to lie for Kr in Rb, according to the chemical arguments mentioned in Sec. I. It is of considerable interest, also, that the absorption and emission profiles have such different shapes, with absorption linear above a slightly rounded threshold, while the emission exhibits very much more broadening, except for the sharp peak itself. These features are discussed further in Sec. IV C.

Both sodium salicylate and CsI detector data are compared in Fig. 7 for the much broader absorption profiles of Xe in K, Rb, and Cs host lattices. The data generally appear much the same as those for Kr in the alkali metals, but with the expected wider scatter. Again the overlap is relatively small, and it occurs precisely in the region 7.6 ± 0.2 eV where chemical arguments predict that the electronically relaxed threshold should lie for Xe in Cs.

In summary we note that the Kr and Xe data both reveal linearlike absorption thresholds and Lorentzian-like emission thresholds that exhibit relatively small overlaps through the exact region predicted by model calculations of the relaxed excited-state energy.[10] Inset in Fig. 7, the emission edges for Xe and Kr in Rb are shown overlaid, with the Kr data shifted but not scaled in energy, to show that the actual shapes and widths of the edges are in fact similar for the two cases.

In recent work[26] we have been able to obtain outer core-hole lifetimes of the heavy alkali metal from a comparison among their relative emission efficiencies. The observed lifetimes and intensities are both determined by the Auger decay rate, which short circuits the much slower photon emission channel. When the relative intensities are corrected for differences among the atomic oscillator strengths, the deduced core-hole lifetimes for K, Rb, and Cs agree with values determined directly from the Fermi edge broadening. In order to apply similar methods to a determination of rare-gas core-hole lifetimes we have measured the rare gas emission intensity relative to that of the alkali host in a number of alloys. Samples for this purpose were made sufficiently thin that reabsorption of the emitted light played no significant role, as described in Sec. II. The type of results achieved

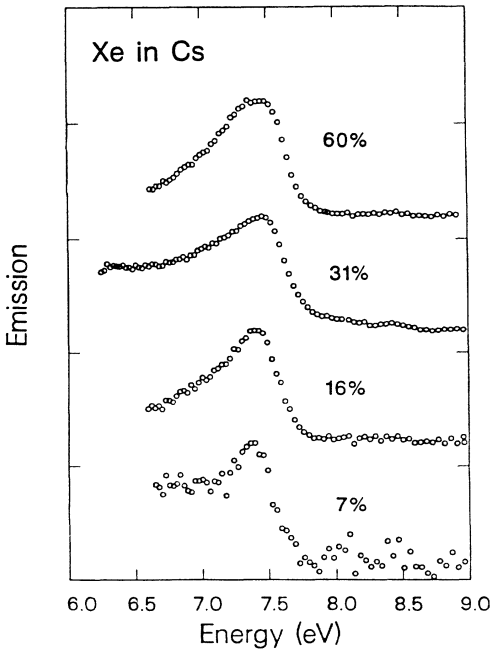

FIG. 5. Emission spectra for various concentrations of Xe in Cs after subtraction of the pure metal background. The data are from thick films using the sodium salicylate detector and were acquired at appreciably higher beam current than all other spectra, as noted in the text.

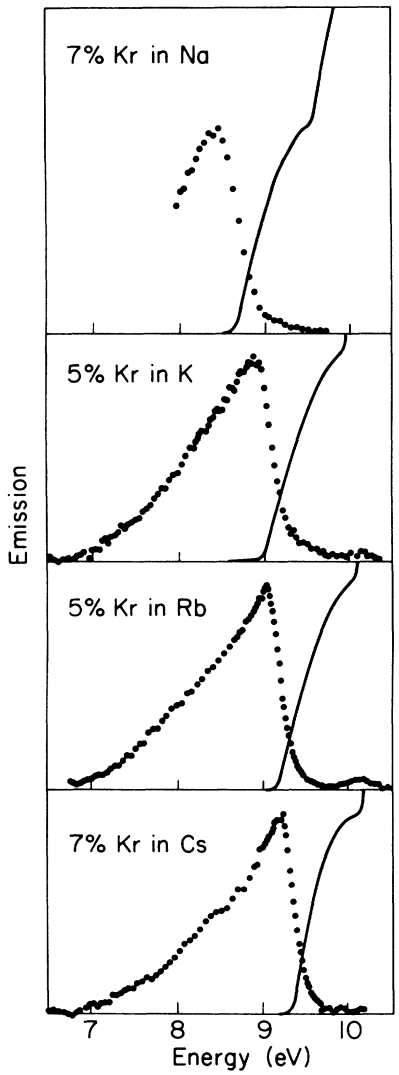

FIG. 6. Emission-band overlap with absorption for Kr near dilution in the alkali metals. Circles: emission data (this work). Solid lines: comparable absorption data from Ref. 10.

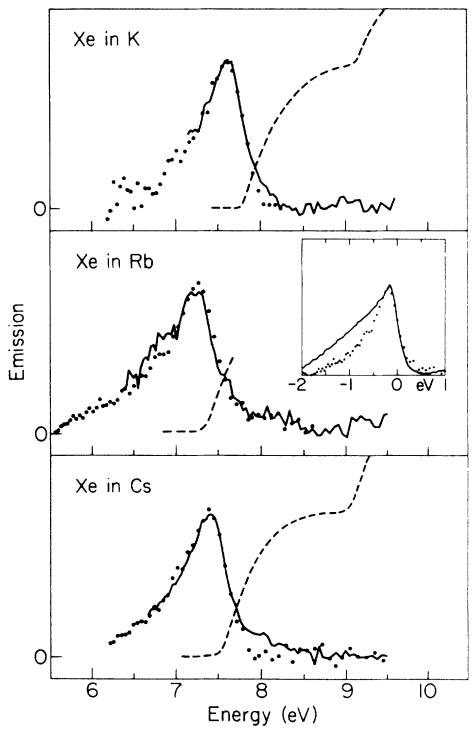

FIG. 7. Emission band overlap with absorption for Xe near dilution in the alkali metals. Circles: emission data using the sodium salicylate detector. Solid lines: emission data using the CsI detector. Dashed lines: comparable absorption data from Ref. 10. Inset shows the emission edges of dilute Kr in Rb (line) and Xe in Rb (circles) overlaid.

here are illustrated in Fig. 8 by the example of Kr observed with Cs in Cs–Kr alloys. Similar results were acquired for both Kr and Xe in K, Rb, and Cs. Figure 9 presents emission strengths for Kr impurities relative to the host alkali band as a function of Kr concentration in

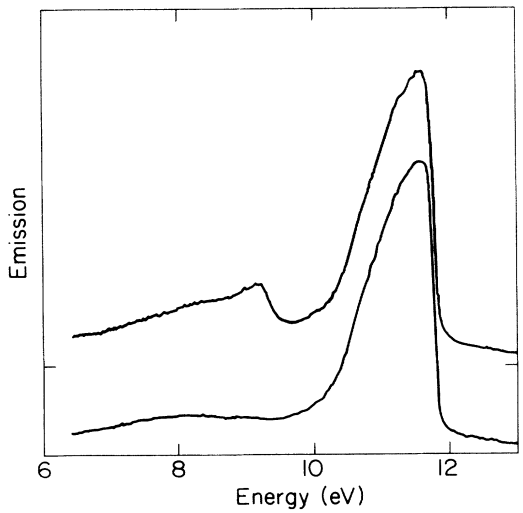

FIG. 8. Top: emission spectrum of 7 at. % Kr in Cs showing the relative magnitude of emission from host and impurity bands. Bottom: emission spectrum of pure Cs. Note the zero offset between spectra.

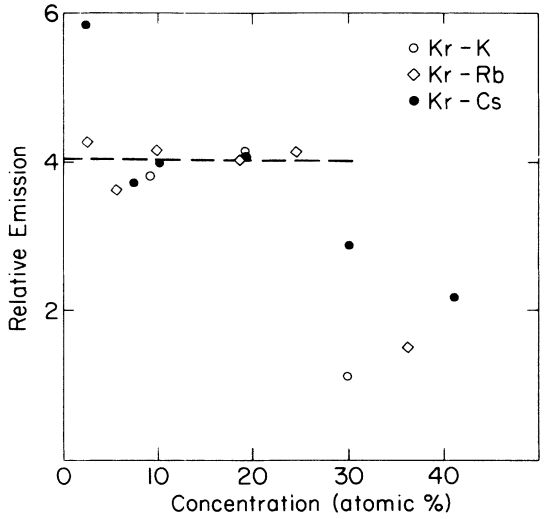

FIG. 9. Emission per atom for Kr impurities in the heavy alkali metals relative to emission per atom of the host metal. The data for Kr in K have been multiplied by a factor of 1.66 and those for Kr in Rb by a factor of 2.68 in order to match the data points for Kr in Cs. Raw spectra were corrected for energy dependence of the photon collection efficiency and scaled by E^{-4} to account for spectrometer resolution and phase-space factors, before comparing areas under the emission bands.

K, Rb, and Cs metals. Data for Kr–K and Kr–Rb have been scaled by factors of 1.66 and 2.68, respectively, to match the Kr–Cs points. It is clear from Fig. 9 that the emission per Kr atom remains essentially constant for concentrations below ~25 at. % Kr. This is an indication that the main emission band is dominated by the decay of excitations associated with single impurity sites, rather than emission from excited levels due to interaction among impurities. Emission per atom from rare-gas dimers, for example, should scale linearly with the concentrations since the number of pairs is proportional to the square of the concentration. This has actually been observed at higher photon energy, as discussed below. Table I summarizes the relative emission strengths from emission data of dilute alloys. As in Fig. 9, the raw data has been corrected for energy dependence of the photon collection efficiency and scaled by E^{-4} to eliminate spectrometer resolution and phase space factors before comparing relative areas under the emission bands. Neither Fig. 9 nor Table I has been adjusted to account for differing atomic oscillator strengths of the different species; another factor of E is included in the oscillator strength by definition. These results are interpreted in terms of core-hole lifetimes in Sec. IV.

The number of additional observations are worth quan-

TABLE I. Ratios of emission intensity per impurity atom relative to emission per atom of the host metal for isolated Kr and Xe impurities in alkali metals.

	K	Rb	Cs
Kr	2.4	1.5	4.0
Xe	5.0	3.1	12.3

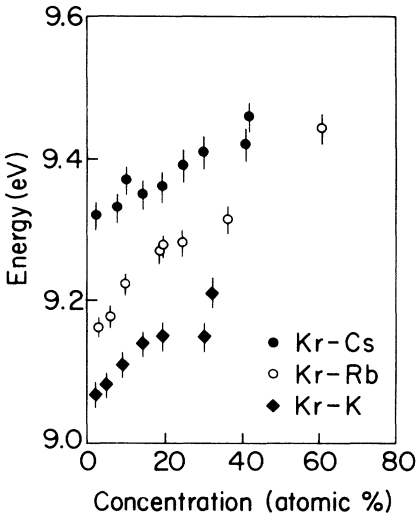

FIG. 10. Threshold energy of the Kr emission band as a function of concentration for Kr in Cs (open circles), Kr in Rb (solid circles), and Kr in K (solid diamonds).

titative summary, although their interpretations remain obscure at the present time. One of these is the rare-gas threshold energy, which differs from one host lattice to the next and also changes with composition in each system. Figures 10 and 11 show these results for Kr and Xe, respectively, in several alkali metals. A second area of interest concerns the pair peaks that appear weakly in the emission spectra of Figs. 2–5. A much larger fraction of absorption strength is observed in these processes than is apparent in the emission results.[11] The Kr pair peaks obtained from thin film samples are presented on an expanded scale in Fig. 12 to make their concentration dependence visible. Particularly for the lowest energy peak there is a systematic variation of intensity with concentration, as shown in Fig. 13. The data point clearly to the origins of this line in rare-gas pairs. It has been thought that these processes arise from a molecular excited configuration of two rare-gas atoms that occupy neighboring sites in the lattice.[11] Their sharpness and symmetric shape is attributed to reduced overlap with the

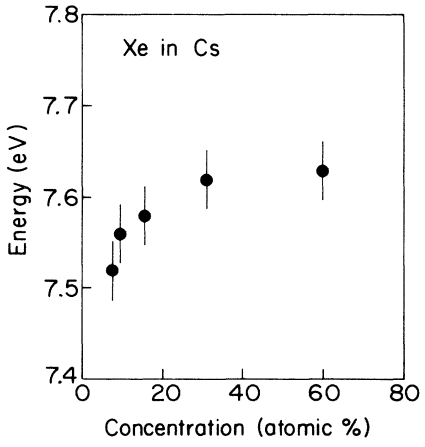

FIG. 11. Threshold energy of the Xe emission band as a function of concentration for Xe in Cs.

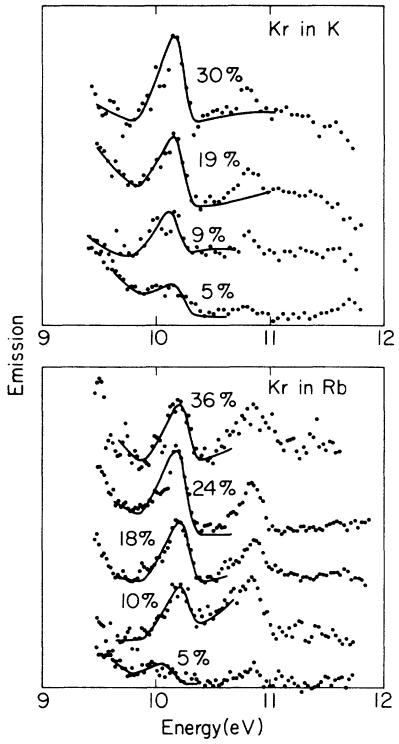

FIG. 12. Emission features arising from the interaction of pairs of Kr impurities in K and Rb for several Kr concentrations. The data are from thin films, as described in Sec. II of the text, and the main Kr emission bands have been normalized to the same area within each data set. Solid lines are fits of a common peak shape plus cubic background to the data.

conduction states, while their weak intensity and the constancy of single impurity emission to high concentration (Fig. 9) suggest that the lifetime of the pair excitation may be dominated by decay into a single excited rare-gas center with a neighboring ground-state impurity. The emission threshold for this configuration will be slightly

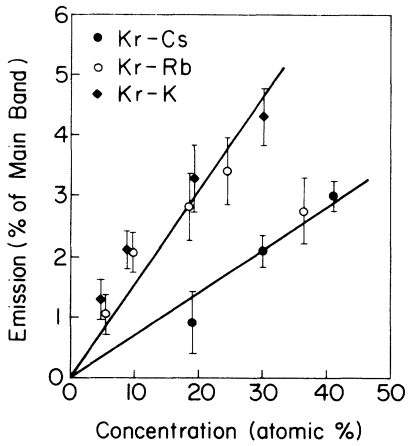

FIG. 13. Low-energy pair peak intensity as a function of Kr concentration as determined by the fits shown in the previous figure. Note that the intensity is given relative to that of the main emission band, which itself scales with concentration.

different from that of a rare-gas atom isolated in the metal matrix, which probably accounts for a shoulder noticeable on the emission edges of some of the higher concentration alloys in Figs. 2–4. A similar analysis of the upper peak intensity is much less revealing. In all, the pair peak behavior of the emission spectra makes satisfactory contact with these processes as observed in absorption, but the emission results are somewhat less striking in their intensity and in their systematics.

IV. DISCUSSION

In this section the experimental results for the rare-gas excited state are analyzed and their significance discussed. Sec. IV A includes a quantitative discussion of the observed spectral line shapes and in Sec. IV B the excited state lifetimes are obtained. These results lead in Sec. IV C to a speculative discussion of the mechanisms that cause the rare-gas excited impurity state to display such unusual spectral characteristics.

A. Band shapes

Figure 7 (inset) establishes that through the region of the emission edges the spectra of Kr and Xe are remarkably similar in shape. They are, however, noticeably different from alkali-metal emission band edges. The differences are made apparent in Fig. 14 where the smoothed Kr band at dilution in Rb is compared with the Rb band itself, the spectra being normalized to identical areas for ease of comparison. One major difference is that the small, mostly Gaussian broadening of the Rb edge is replaced for Kr by a broader, more Lorentzian profile. A second difference in the overall shapes of the bands is in the threshold peak structure. For Rb the threshold peak is quite narrow and it appears clearly superposed on a remaining bandshape that curves over at high energy much as expected for the one-electron transition strength to an s-like band state density. A calculated transition strength of this type[29] for Na is indicated by the dashed line in Fig. 14, and analogous results for potassium[30] confirm that similar behavior is expected for all the alkali metal. Such modeling has no quantitative significance for alkalis, because the core hole seriously distorts the local electronic structure, but it nevertheless retains some qualitative validity. In contrast, the Kr band in Fig. 14 rises progressively faster with increasing energy so that no distinction between the peak and the underlying band is possible. Both the Kr and Rb bands exhibit extended low-energy tails that arise from fast scattering of the *band* hole present in the final state. Model fits to the Kr band, described below, determine this scattering rate to be similar for both impurity and host excitations.

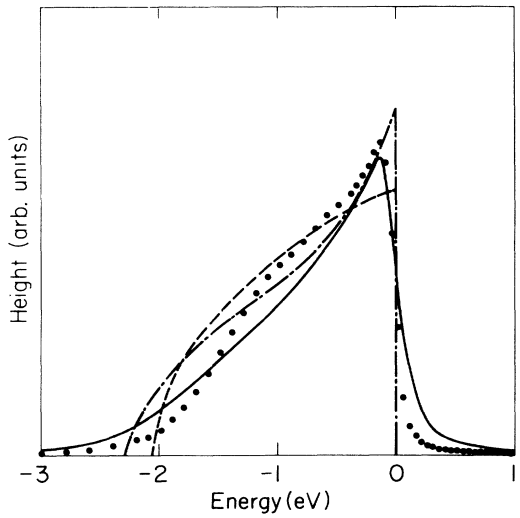

FIG. 14. Solid line: Kr emission band from 5 at. % Kr in Rb. Circles: emission band of pure Rb. Dashed line: calculated transition strength for Na scaled to the Rb free electron bandwidth. The transition density of states calculated in Ref. 29 has been multiplied by a factor E^3 to enable direct comparison with the photon emission spectra. Dash-dotted line: calculated one-electron emission spectrum from Ref. 15. All spectra have been normalized to equal area for comparison.

It should be recalled here that the emission bands of the four alkalis Na–Cs exhibit very similar general shapes when scaled to a common energy width.[26] Systematic differences are apparent only in the small MND threshold peak which dwindles through the series to become unobservably small for Cs. The present data do not establish clearly that the rare gases conform to a similar scaling behavior. Their edges are very similar, but the Xe band appears much narrower than that of Kr. With the detection difficulties present in the band tail for Xe, it is difficult to obtain a reliable assessment of the response in this region, relative to that of Kr.

It is of particular interest that the excited rare-gas atom takes the $np^5(n+1)s$ structure that fits smoothly into an $np^6(n+1)s$ alkali-metal ground state, so that the excited configuration in the alloy produces an almost uniform electron liquid. Therefore the recombination spectra may be expected to resemble those anticipated for the alkalis themselves before the perturbing effect of the localized core hole was recognized. This excited state is shown schematically in Fig. 15. Also shown there is the ground state in which the neutral rare-gas atom repels the conduction electrons from its vicinity to leave a vacancylike electron distribution. As recalled in Sec. I,

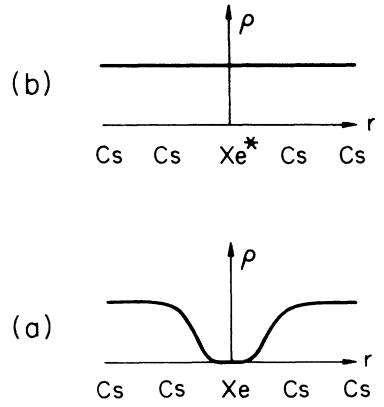

FIG. 15. Conduction-electron density distributions near the rare-gas impurity center in its (a) ground and (b) excited state.

these structures reproduce the ground-state resistivity[9] and the observed core excitation energy (Sec. III). Also they predict[10] phase-shift changes that give the MND exponent $\alpha=0.35\pm0.1$ as compared to detailed electronic structure calculations that give values ranging between 0.28 and 0.35 for various rare-gas–alkali-metal systems.[15] Accordingly, the general features shown in Fig. 15 may be regarded as securely established.

The calculations of electronic structure cited above included calculations of the transition density of states between the core-excited Kr atom in Rb and the final ground state reached after emission. This corresponds to a prediction of the emission profile in the absence of many-body anomalies near E_F. For this purpose the theory employed the Korringa-Kohn-Rostoker (KKR) approach within the coherent-potential approximation (CPA) to the alloy electronic structure, carried through to self-consistency in the potentials and charge distributions. In fact the emission band so determined differs markedly from the density of host metal band states. The KKR-CPA result for Kr in Rb is shown in Fig. 14 appropriately scaled for comparison with the other curves. This prediction is noticeably more weighted towards state density near E_F than is the Na "band-theory" curve, apparently due to more d-symmetry states at the impurity site.[31]

To study detailed fits to the data we have modified the KKR-CPA predictions by a threshold enhancement using an MND prescription with an exponent $\alpha=0.14$. This choice was dictated by the fit to the data, but may be justified in part by the calculated $\alpha\sim0.3$ and by the observed fact that exponents measured in emission tend to be smaller than those from absorption, which in turn are usually comparable with predicted values.[32,20,21] Final-state lifetime broadening identical to that required to fit the Rb band[26] was also incorporated in the model. This contributes negligibly to the edge width, since quasiparticle lifetimes are infinite at E_F, but does broaden the band tail. The resulting band is illustrated by a broken line in Fig. 16. To best fit the data for Kr in Rb, shown by open circles, this curve was shifted into coincidence with the observed threshold energy and broadened by a Lorentzian contribution of width 180 meV and a Gaussian of width 100 meV. In making these model fits we do not, in the first place, associate the Gaussian or Lorentzian components of the broadening with specific mechanisms, such as phonons or state lifetimes, leaving these questions for the later discussion. Fits of comparable quality were obtained for Gaussian components in the range 0–100 meV and with somewhat broader Lorentzians. The model did not include emission from the N_2 spin-orbit partner, since this is apparently shorted out by fast Coster-Kronig decay. Inclusion of a properly broadened [see Eq. (1) of Ref. 26] and shifted N_2 band revealed that the best fits were indeed with negligible spin-orbit intensity, and that this emission could be no more than $\sim6\%$ of the main band to maintain an acceptable fit. Even at this level of N_2 emission, the required Lorentzian component was always >0.12 eV and the Gaussian contribution <0.15 eV. The resulting fit to the data in Fig. 16 is quite good overall, and especially so near the edge. One feature that

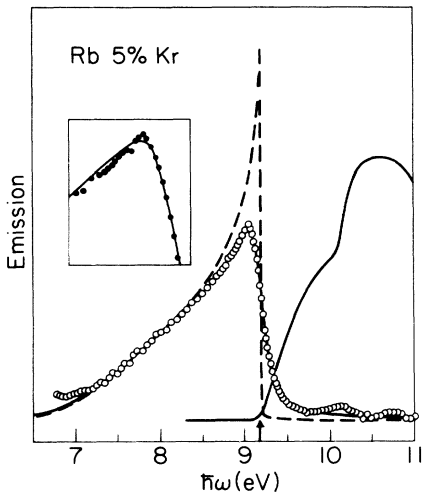

FIG. 16. Kr emission in Rb for the concentration indicated, together with the comparable absorption results (Ref. 10). The line through the emission data points is the theory shape (dashed line) convolved with a lifetime width of 180 meV and a 100-meV Gaussian component. Note the common threshold of absorption and unbroadened emission, close to the predicted position (arrow). Inset is a blowup of the threshold peak.

remains noticeably incorrect, however, is the peak itself. The expanded figure shown inset demonstrates that the measured peak is several times sharper than the 180-meV Lorentzian permits. This apparent paradox is a challenge to theory because it is not possible for a broadened curve to exhibit sharper features than those of the convolving function that causes the broadening. We return to this particular question below, in Sec. IV C.

An important result revealed by Fig. 16 is that the unbroadened theoretical band, when shifted for a best fit to the data, has a threshold edge that coincides very closely with the absorption threshold. Both are well within the stated uncertainty of the threshold energy predicted by chemical modeling. This location for the emission edge is rather independent of the assumed bandshape. Any sharp cutoff that can be broadened by convolution to fit the data must, in fact, lie close in energy to the experimental emission half height. Thus the important conclusion that the two thresholds closely coincide is not very sensitive to the detailed modeling. If the 180-meV Lorentzian is now associated with lifetime broadening, the model is consistent with the absence of a Stokes shift between the two thresholds because the excited-state lifetime is so short compared with the relevant phonon frequencies ($\hbar\omega_D\leq10$ meV). The predicted phonon widths of the rare-gas core excitations in heavy alkali metals are 30–40 meV of Gaussian broadening (FWHM).[33] This seems reasonably consistent with the data fit described above, which requires a Gaussian component in the range 0–100 meV. However, in the following section we provide evidence that a simple interpretation of the emission edge width as just described may be incorrect.

B. Core-hole lifetimes

When alkali-metal cores are excited, the relative core-hole lifetimes can be derived from measurements of the

total emission strengths. The values so obtained agree well with the widths of the Lorentzian component of Fermi edge broadening determined directly by fits to the observed edge profile at various temperatures.[26] It is necessary to scale the observed emission rates by their atomic oscillator strengths and an additional factor E^2, in order to eliminate from the comparison those factors that are intrinsic to the photon emission process. After also accounting for the relative excitation cross sections, we are left with a comparison of the Auger rates that actually determine the lifetimes, since they are several orders of magnitude faster than the photon rate. In practice it is necessary to use theoretical oscillator strengths because many of the actual values are not yet available. Even so, quite satisfactory lifetime determinations have been made in this way.[26]

For the present study, we have used oscillator strengths calculated by McGuire[34] in *LS* coupling for both the rare gas and alkali atoms. The values are 0.097, 0.146, and 0.141 for the $np^6(n+1)s \rightarrow np^5(n+1)s^2$ transitions in K ($n=3$), Rb ($n=4$), and Cs ($n=5$), respectively, while for Kr $4p^6 \rightarrow 4p^5 5s$ it is 0.277, and 0.381 for Xe $5p^6 \rightarrow 5p^5 6s$. For the rare gases these values reproduce the experimental results[35,36] (summed over J sublevels) to an accuracy better than 30%, and trends within the series Ar–Xe are reproduced to ~15%. Similarly, the calculated alkali oscillator strengths (no experimental data exist) relative to the rare gases should be accurate to about 15%. A further complication comes from the spin-orbit coupling in these atoms. Essentially all of the emission signal results from transitions to the $^2P_{3/2}$ core hole in both the rare gases and alkali metals. Consequently, the *LS* oscillator strengths, appropriate for the entire p shell, must be weighted by suitable degeneracy factors to account for only these transitions. Kr and Xe terms are well approximated by pure *j-j* coupling, as judged by the near equality of experimental oscillator strength for transitions from both the $^2P_{1/2}$ and $^2P_{3/2}$ core holes. The neighboring alkalis metals Rb and Cs must also conform to this description. Ar and K are better treated in an intermediate coupling scheme, but *j-j* coupling will be used here for the sake of simplicity. In the alkali metals, there are four allowed transitions to the $J=\frac{3}{2}$ excited state and only two to the $J=\frac{1}{2}$ level, therefore we take the oscillator strength for transitions to $J=\frac{3}{2}$ to be $\frac{4}{6}$ of the *LS* value. Similarly, the rare gases have three allowed transitions to a $J=1$ excited state with a $^2P_{3/2}$ core hole, and three more to the $J=1$ state associated with a $^2P_{1/2}$ core hole. The f value for transitions filling the $^2P_{3/2}$ hole is therefore taken as $\frac{3}{6}$ the calculated result for *LS* coupling. For each component of the alloy, the total emission intensity was assumed to conform to Eq. (2) of Ref. 26. We note, however, that the excitation cross sections $\sigma_{1/2}$ and $\sigma_{3/2}$ in this formula must be interpreted as relative probabilities for creation of *optically allowed* excited configurations with $^2P_{1/2}$ or $^2P_{3/2}$ core holes. All $np^5(n+1)s^2 \rightarrow np^6(n+1)s$ transitions of the alkali metals are allowed, so electron-excitation cross sections from Bethe's formula were used directly. In the rare-gas case for $np^5(n+1)s \rightarrow np^6$, the fraction of allowed transitions is $\frac{3}{8}$ for the $^2P_{3/2}$ core hole, and $\frac{3}{4}$ for the $^2P_{1/2}$ hole. The cross sections for core-hole creation were therefore scaled by these factors before use in Eq. (2) of Ref. 26. For the rare gases and Cs we take the Coster-Kronig rate W' to be much larger than the Auger rate W. The same approximation produces only ~5% change in the results found for K and Rb hosts.

From the relative emission data, using the methods just described, we obtain apparent Auger lifetimes τ for Xe that are respectively 3.4, 4.0, and 21.2 times longer than the host metal core lifetime for K, Rb, and Cs based dilute solutions. For Kr the analogous ratios are 3.0, 3.4, and 12.2. Our earlier results for the pure alkali metals identify their core-hole lifetime widths $\hbar/\tau$, as K: 14 meV, Rb: 22 meV, and Cs: 58 meV. On scaling these widths by the lifetime ratios found above we determine the impurity lifetimes presented in Table II. Within the considerable uncertainties it is apparent that Kr and Xe have quite similar lifetimes against Auger decay, and that these show little variation from one host lattice to the next. Indeed, an impurity lifetime width of about 5 meV approximates the results shown in Table II for all the systems studied. This value is apparently well substantiated, since it is obtained from six separate alloy systems that yield results in good mutual consistency. In a preliminary publication,[27] the rare-gas oscillator strengths were taken with different statistical factors and shorter lifetimes near 10 meV were deduced. The present values are to be preferred. Note that in either case the deduced lifetime is substantially less than the 180-meV Lorentzian broadening obtained from the edge fit in Fig. 16. Thus, unlike the case for alkali metals, the absolute emission does not appear to be consistent with the Fermi edge broadening. A proposed explanation of this discrepancy is described in the following section.

C. Excited-state structure

In our efforts to model the excited rare-gas configuration we have encountered several significant inconsistencies. One global point is that the emission and absorption processes lack the normal mirror symmetry about their thresholds, despite the fact that a relaxed threshold is apparently observed and, indeed, its energy can be predicted quite accurately. We are not aware of any other case in which this common symmetry is so clearly absent. No model of the excitation process is available at present to account for both the emission and absorption line shapes. In addition to this difficulty, the Fermi edge in emission is not sharp but instead appears to be lifetime broadened by nearly 200 meV. The

TABLE II. Lifetime widths in meV for Kr and Xe in the heavy alkalis as deduced from relative emission intensities. Error limits have been estimated from uncertainties in the oscillator strengths, in measurement of relative areas, and in the host lifetimes (Ref. 26).

	K	Rb	Cs
Kr	5.0±3.0	6.5±2.0	5.0±2.0
Xe	4.0±3.5	5.5±2.0	3.0±1.5

difficulty here is that nearby features of the spectrum are too sharp by a factor of 3 or more to be consistent with any such broadening. Finally, the lifetime of the excited state as measured by the total emission intensity is too long by more than a factor of 30 to be consistent with the deduced 200-meV Lorentzian width.

In connection with the emission edge width, two points require immediate recognition. First, for the available rate of decay by photon emission, the observed emission intensity requires that the excited initial state persists and emits for a period longer than that for the alkali host excitations. The excited state therefore cannot introduce a 200-meV lifetime width. Nor can the final state cause this broadening, since the process occurs near the Fermi edge where the rare-gas ground state offers no excitations less than several eV and where quasiparticle excitations are too long lived. Therefore some temporal or spatial smearing of the transition energy must take place to cause the line shape.

Second, the evidence is compelling that spatial inhomogeneity, from one site to the next in the lattice, plays no significant role in the large observed width of the rare-gas emission edges. The results in Figs. 2–5 show unambiguously that the edge shape remains much the same over the range ~0-50% rare gas in a variety of systems for two rare-gas species and three alkalis. These span a very wide variety of mean rare-gas environments for which the consequences of spatial inhomogeneity would be expected to vary to a comparable extent. The edge spectra, to the contrary, appear quite insensitive to these changes of environment.

Lacking lifetime or inhomogeneous broadening mechanisms, the observed emission edge width must be due to lattice or electronic relaxation processes. The longitudinal Debye frequencies of 4–10 meV for the host metals are comparable with the rare-gas lifetime width, ~5 meV, as determined by the emission strength. Therefore the emission from these systems must certainly be affected by partial lattice relaxation in addition to the normal width from phonon broadening.[37,38] In partial relaxation, emission can occur at all stages of lattice relaxation since the core-hole lifetime is comparable to the characteristic phonon period. This smears the emission intensity over an energy range roughly twice the lattice relaxation energy of the excited state. With the present revision of the rare-gas excitation lifetimes to ~5 meV, partial lattice relaxation becomes more interesting as a possible explanation of the emission profiles. From a previous theory[33] we estimate the lattice relaxation energy for Kr in K, Rb, and Cs to be 123, 84, and 50 meV, respectively, with corresponding values for Xe about 50% larger. The lifetime-independent part of the phonon width, which roughly adds in quadrature, has been estimated to be 30–40 meV.[33] The broadening expected from partial lattice relaxation is thus comparable with the observed emission edge width. Spectral functions associated with this mechanism are beneved to exhibit an asymmetric tail that can mimic part of the Lorentzian width found in the model fits described above. Also, the sharp peak on the emission spectrum could possibly be explained by contributions from those decay events that occur near the point of full relaxation. Finally, the expected Stokes shift of ~100 meV between absorption and emission may fall within the uncertainties of matching spectra from different spectrometers and locating the unbroadened thresholds.

Within this limited context it would be reasonable to attempt fits of the data to one-electron models, including MND threshold enhancement, and the additional edge broadening due to partial lattice relaxation. This underscores the importance of core-hole lifetime determinations by means independent of line shapes. However, no such model can describe the absorption spectra, particularly since lattice relaxation cannot contribute to the absorption line shape. The striking absence of any threshold enhancement is contrary to theoretical predictions[15] (even considering the contribution of d states,[16] since the associated threshold exponent is only -0.08 using the phase shifts from Ref. 15) and in marked contrast with the emission results reported here. Like the emission characteristics, the absorption anomalies occur in a wide range of materials, and for impurities both in the bulk[10] and on metal surfaces.[12] This indicates that the phenomena are both robust and rather general. The remaining challenge is to construct an explanation that simultaneously accounts for both the emission and absorption observations.

A likely origin for the unexpected behavior lies in the detailed structure of the rare-gas atom in its excited state. The lowest excited level of the rare-gas atom has $J=2$ and is optically forbidden. For atomic Kr and Xe it lies a little less than 100 meV below the optical $J=1$ level.[39] We visualize that the optical state created by photon absorption may evolve into an appropriate admixture over the course of a time interval that is related to the spin flip that transforms $J=1$ into $J=2$. The evident stability of the process suggests that it is local and in part coherent, and that it changes rather slowly with the character of the local metallic environment. We conjecture that these dynamical processes modify the absorption to its observed anomalous form. Emission can take place at any time during the electronic relaxation or after. This may contribute significantly to the broadened edge but still allows the sharp peak to be contributed by processes on the scale of the 5-meV lifetime in the final local state.

The mechanism described above has features in common with the Fano effect in spectroscopy[40] and with the Kondo effect in the spin dynamics of impurities in metals. Similar ideas are obviously contained in the MND problem for a spin-dependent potential. A substantial body of existing research on this latter topic, reviewed by Almbladh and Hedin,[41] is unfortunately lacking a definitive resolution. From the Fano viewpoint we imagine optical and nonoptical excited atomic levels of the rare gas are spread into overlapping continua by interaction with the metallic environment. Then the forbidden levels interfere with and suppress the threshold of the optically allowed continuum, thereby presumably causing the anomalous absorption. The phenomena we have described above may then follow from the subsequent evolution of the coupled-valence–core-hole system, with the eventual decay of the core hole.

V. SUMMARY

We have presented vuv emission spectra from the $np^5(n+1)s \rightarrow np^6$ transitions of core-excited Xe ($n=5$) and Kr ($n=4$) randomly dispersed in alkali-metal host lattices. Interest centers on spectral properties of rare-gas atoms isolated within the metal matrix; "pair peaks" observed at higher concentrations reproduce trends seen in absorption.[11] Emission data from dilute alloys exhibit an unusual relationship to absorption that leads us to suggest a description of the rare-gas excited state that includes the exchange interaction with the core hole. The anomalous line shape of the absorption threshold is attributed to configuration interaction in the excited state, as distinct from the recoil of conduction electrons previously supposed.

The emission and absorption threshold profiles are quite different and lack the usual mirror symmetry between the edges, even though the spectra seem to share a common threshold energy. By detailed modeling we find that the entire emission band is adequately described in a "change in self-consistent field" (ΔSCF) model, including MND enhancement, but is broadened by the lifetime of the band hole of the final state, and also by an additional contribution, largely described by the Lorentzian component in our chosen model. The analogous model for absorption fails to provide even a qualitative fit to that line shape. Reliable arguments predict the common threshold energy to within 2% of the observed values.

In some cases the experimental emission spectrum (e.g., from dilute Kr in Rb) is very sharply peaked at the emission maximum. This well-resolved feature is clearly inconsistent with the nearly 200 meV of observed Lorentzian broadening of the emission edge. Thus the bulk of the edge width cannot be due to core-hole lifetime broadening. Measurements of emission intensity under the rare-gas band relative to that from the host metal are consistent with this conclusion. They reveal a lifetime width of ~5 meV for Xe or Kr in each of the heavy alkali metals, K, Rb, and Cs. This is almost a factor of 40 too small to account for the observed edge broadening. One possible source for the emission edge width is partial lattice relaxation in the excited state, since the 5-meV lifetime is comparable with the host phonon frequencies, and the sharp peak may then be due to emission events occurring near complete relaxation. It is apparent, however, that equivalent one-electron models cannot reproduce *both* the emission and absorption edge shapes from a common near-edge electronic structure. In particular, MND enhancement of the absorption threshold, while predicted to be much stronger than that observed in emission, is instead completely absent. We have therefore examined the possibility that the rare-gas state reached by excitation differs from that responsible for the observed emission.

Since chemical modeling of the ground and excited configurations is successful in predicting the energetics, it cannot be far from correct. We speculate that details of the excited configuration may be important and, specifically, that exchange between conduction electrons and the core hole must be included. This interaction causes a core-excited rare-gas atom to differ from its $Z+1$ analog, a ground-state alkali atom, by splitting of the valence s level into two different angular momentum states, only one of which is optically accessible. Within the metallic environment these two levels spread into separate continua coupled by a matrix element related to the spin-flip scattering rate. Interference between the optically allowed and forbidden levels suppresses the absorption intensity at the threshold, as in a Fano antiresonance for a discrete state interacting with a continuum. In this picture, emission takes place both during and after electronic relaxation, perhaps contributing to both the large edge width and the sharp peak observed in the emission.

Lacking adequate theory this proposed explanation must remain speculative. Regardless of details, however, the final explanation of these anomalous line shapes is likely to center on configuration interactions that suppress the intrinsic edge shape expected from electron recoil. Note that other low valence impurities alloyed into simple metals exhibit absorption profiles that clearly do exhibit the characteristic interference between a discrete state and the electronic continuum.[42–44] Plausible fits to the absorption spectra from rare-gas impurities can also be obtained using a Fano line shape at threshold (although this requires a discrete localized excited level that is optically forbidden). Recent work[26–28] has pointed to trends in the $np^5(n+1)s^2 \rightarrow np^6(n+1)s$ Auger lifetimes of the alkali metals, also, that are difficult to explain within a one-electron model. It therefore appears possible that the effects of local configuration interaction on core excitation may be ubiquitous among "simple" metallic systems.

ACKNOWLEDGMENTS

We wish to thank R. L. Fink, A. Matheny, and C. Gutleben for invaluable assistance and discussions during the course of this work. In addition, we are grateful to D. E. Meltzer and E. J. McGuire for communication of their results prior to publication. This research was supported in part by the National Science Foundation under Grant No. DMR 86-01593. Use was made of Materials Research Laboratory facilities supported by Grant No. DMR 86-12860.

---

*Present address: National Institute of Standards and Technology (formerly National Bureau of Standards), Gaithersburg, MD 20899.

[1] J. C. P. Mignolet, J. Chem. Phys. **21**, 1298 (1953).

[2] G. Ehrlich and F. G. Hudda, J. Chem. Phys. **30**, 493 (1959); R. Gomer, Aust. J. Phys. **13**, 391 (1960); C. Mavroyannis, Mol. Phys. **6**, 593 (1963); T. Engel and R. Gomer, J. Chem. Phys. **52**, 5572 (1970), and Ref. 4.

[3] J. E. Cunningham, D. K. Greenlaw, and C. P. Flynn, Phys. Rev. B **22**, 717 (1980).

[4]C. P. Flynn and Y. -C. Chen, Phys. Rev. Lett. **46**, 447 (1981); Y. -C. Chen, J. E. Cunningham, and C. P. Flynn, Phys. Rev. B **30**, 7317 (1984).
[5]N. D. Lang, A. R. Williams, F. J. Himpsel, B. Reihl, and D. E. Eastman, Phys. Rev. B **26**, 1728 (1982).
[6]K. Shinjo, S. Sugano, and T. Sasada, Phys. Rev. B **28**, 5570 (1983).
[7]M. Tsukada and W. Brenig, Z. Phys. B **57**, 297 (1984).
[8]B. Raz, A. Gedanken, U. Even, and J. Jortner, Phys. Rev. Lett. **28**, 1643 (1972). See also N. Schwentner, E. -E. Koch, and J. Jortner, *Electronic Excitations in Condensed Rare Gases* (Springer-Verlag, Berlin, 1985), and references therein.
[9]D. J. Phelps, R. Avci, and C. P. Flynn, Phys. Rev. Lett. **34**, 23 (1975); D. J. Phelps and C. P. Flynn, Phys. Rev. B **14**, 5279 (1976).
[10]R. A. Tilton, D. J. Phelps, and C. P. Flynn, Phys. Rev. Lett. **32**, 1006 (1974); D. J. Phelps, R. A. Tilton, and C. P. Flynn, Phys. Rev. B **14**, 5254 (1976).
[11]R. A. Tilton and C. P. Flynn, Phys. Rev. Lett. **34**, 20 (1975); R. A. Tilton, D. J. Phelps, and C. P. Flynn, Phys. Rev. B **14**, 5265 (1976).
[12]Doon Gibbs, J. E. Cunningham, and C. P. Flynn, Phys. Rev. B **29**, 5292 (1984).
[13]T. -C. Chiang, G. Kaindl, and D. E. Eastman, Solid State Commun. **41**, 661 (1982); G. Kaindl, T. -C. Chiang, D. E. Eastman, and F. J. Himpsel, Phys. Rev. Lett. **45**, 1808 (1980).
[14]K. Jacobi and H. H. Rotermund, Surf. Sci. **116**, 435 (1982); H. H. Rotermund and K. Jacobi, *ibid.* **126**, 32 (1983).
[15]D. E. Meltzer, F. J. Pinski, and G. M. Stocks, Phys. Rev. B **37**, 6011 (1988).
[16]For recent reviews, see J. W. Wilkins, in *X-Ray and Atomic Inner-Shell Physics, University of Oregon, Eugene, Oregon, 1982,* AIP Conf. Proc. No. 94, edited by B. Crasemann (AIP, New York, 1982), p. 687, and Ref. 34.
[17]G. D. Mahan, Phys. Rev. B **163**, 612 (1967).
[18]P. Nozieres and C. T. DeDominicis, Phys. Rev. B **178**, 1097 (1969).
[19]P. W. Anderson, Phys. Rev. Lett. **18**, 1049 (1967).
[20]G. W. Bryant, Phys. Rev. B **19**, 2801 (1979).
[21]P. H. Citrin, G. K. Wertheim, and M. Schluter, Phys. Rev. B **20**, 3067 (1979), and references therein.
[22]R. C. Kittler and L. M. Falicov, Solid State Commun. **20**, 973 (1976).
[23]H. Kaga, Phys. Lett. **67A**, 431 (1978); H. Kaga and J. D. Dow, J. Phys. Soc. Jpn. **45**, 1261 (1978).
[24]M. A. Bowen, D. V. Froelich, and J. D. Dow, Phys. Lett. **102A**, 73 (1984).
[25]H. W. B. Skinner, Philos. Trans. R. Soc. London, Ser. A **239**, 95 (1940).
[26]R. L. Fink, P. N. First, and C. P. Flynn, Phys. Rev. B **38**, 5839 (1988).
[27]P. N. First, R. L. Fink, and C. P. Flynn, Phys. Rev. Lett. **60**, 952 (1988).
[28]R. L. Fink and C. P. Flynn (unpublished).
[29]R. P. Gupta and A. J. Freeman, Phys. Lett. **59A**, 223 (1976).
[30]T. McMullen, J. Phys. C **3**, 2178 (1970).
[31]G. D. Mahan, in *Fermi Surface Effects,* edited by J. Kondo and A. Yoshimori (Springer-Verlag, Berlin, 1988).
[32]T. A. Callcott, E. T. Arakawa, and D. L. Ederer, Phys. Rev. B **18**, 6622 (1978).
[33]C. P. Flynn, Phys. Rev. Lett. **37**, 1445 (1976).
[34]E. J. McGuire (private communication).
[35]W. B. Westerveld, Th. F. A. Mulder, and J. Van Eck, Quant. Spectrosc. Radiat. Transfer **21**, 533 (1979).
[36]E. Matthias, R. A. Rosenberg, E. D. Poliakoff, M. G. White, S. -T. Lee, and D. A. Shirley, Chem. Phys. Lett. **52**, 239 (1977).
[37]C. -O. Almbladh, Phys. Rev. B **16**, 4343 (1977).
[38]G. D. Mahan, Phys. Rev. B **15**, 4587 (1977).
[39]C. E. Moore, *Atomic Energy Levels,* Natl. Bur. Stand. Ref. Data Ser., Natl. Bur. Stand. (U.S.) Circ. No. 35 (U.S. GPO, Washington, DC, 1971).
[40]L. N. Oliveira and J. W. Wilkins, Phys. Rev. B **32**, 696 (1985).
[41]C. -O. Almbladh and L. Hedin, in *Handbook of Synchrotron Radiation,* edited by E. -E. Koch (North-Holland, Amsterdam, 1983).
[42]R. Avci and C. P. Flynn, Phys. Rev. Lett. **37**, 864 (1976); R. Avci and C. P. Flynn, Phys. Rev. B **19**, 5981 (1979).
[43]T. H. Chiu and C. P. Flynn, Phys. Rev. B **33**, 5202 (1985).
[44]T. McMullen and B. Bergersen, Can. J. Phys. **50**, 1002 (1972).